

# SH3-binding Protein 5 Mediates the Neuroprotective Effect of the Secreted Bioactive Peptide Humanin by Inhibiting c-Jun NH<sub>2</sub>-terminal Kinase\*

Received for publication, March 15, 2013, and in revised form, July 12, 2013. Published, JBC Papers in Press, July 16, 2013, DOI 10.1074/jbc.M113.469692

Yuji Takeshita<sup>‡S1</sup>, Yuichi Hashimoto<sup>‡1</sup>, Mikiro Nawa<sup>‡</sup>, Hiroyuki Uchino<sup>§</sup>, and Masaaki Matsuoka<sup>‡2</sup>

From the <sup>‡</sup>Department of Pharmacology, Tokyo Medical University, 6-1-1 Shinjuku, Shinjuku-ku, Tokyo 160-8402, Japan and the <sup>§</sup>Department of Anesthesiology, Tokyo Medical University, 6-7-1 Nishi-Shinjuku, Shinjuku-ku, Tokyo 160-0023, Japan

**Background:** Humanin, a secreted bioactive peptide, suppresses a variety of cell toxicities.

**Results:** An intracellular protein SH3BP5, which directly inhibits JNK activity, is identified as an effector of Humanin.

**Conclusion:** SH3BP5 is a physiological inhibitor of JNK and the firstly identified effector of Humanin.

**Significance:** The discovery provides a novel mechanistic insight into the actions of JNK and Humanin.

Humanin is a secreted bioactive peptide that suppresses cell toxicity caused by a variety of insults. The neuroprotective effect of Humanin against Alzheimer disease (AD)-related death is mediated by the binding of Humanin to its heterotrimeric Humanin receptor composed of ciliary neurotrophic receptor  $\alpha$ , WSX-1, and gp130, as well as the activation of intracellular signaling pathways including a JAK2 and STAT3 signaling axis. Despite the elucidation of the signaling pathways by which Humanin mediates its neuroprotection, the transcriptional targets of Humanin that behaves as effectors of Humanin remains undefined. In the present study, Humanin increased the mRNA and protein expression of SH3 domain-binding protein 5 (SH3BP5), which has been known to be a JNK interactor, in neuronal cells. Similar to Humanin treatment, overexpression of SH3BP5 inhibited AD-related neuronal death, while siRNA-mediated knockdown of endogenous SH3BP5 expression attenuated the neuroprotective effect of Humanin. These results indicate that SH3BP5 is a downstream effector of Humanin. Furthermore, biochemical analysis has revealed that SH3BP5 binds to JNK and directly inhibits JNK through its two putative mitogen-activated protein kinase interaction motifs (KIMs).

Humanin was originally identified as a short peptide that inhibited Alzheimer disease (AD)<sup>3</sup>-related neuronal death (1,

\* This work was supported in part by the Grant-in-aid for Scientific Research (B) (Grant 23390059) (to M. M.), the Promotion of Science and Technology project for private universities, with a matching fund subsidy from the Ministry of Education, Culture, Sports, Science, and Technology (MEXT) (to M. M.), and the Grant-in-Aid for Scientific Research (C) (Grant 25460343) (to Y. H.).

<sup>1</sup> Both authors contributed equally to this work.

<sup>2</sup> To whom correspondence should be addressed: Department of Pharmacology, Tokyo Medical University, 6-1-1 Shinjuku, Shinjuku-ku, Tokyo 160-8402, Japan. Tel.: 81-3-3351-6141; Fax: 81-3-3352-0316; E-mail: sakimatu@tokyo-med.ac.jp.

<sup>3</sup> The abbreviations used are: AD, Alzheimer disease; A $\beta$ , amyloid  $\beta$ ; APP, amyloid  $\beta$  precursor protein; Btk, Bruton's tyrosine kinase; caASK1, constitutively active apoptosis signal-stimulating kinase-1; caJNK, constitutively active JNK; htHNR, heterotrimeric Humanin receptor; HN, Humanin; HNG, Humanin G (S14G-Humanin); JIP-1, JNK-interacting protein-1; PHN, primary mouse hippocampal neuron; p-JNK, phosphorylated JNK; KIM, mito-

gen-activated protein kinase interaction motif; Sab, SH3 domain-binding protein that preferentially associates with Bruton's tyrosine kinase Btk; SH3BP5, SH3 domain-binding protein 5; SH3BD, SH3-binding domain.

2). Since then, multiple studies have shown that Humanin inhibits cell death in cell-based AD-related neuronal death models *in vitro* (Refs. 2–4 for review). Humanin also suppresses cell death in a variety of non-AD-related *in vitro* and *in vivo* cell death models; for example, serum deprivation-induced death of several cell types including PC12 neuronal cells (5), primary peripheral lymphocytes (6), K562 myeloblasts (7), and cultured islet  $\beta$  cells (8), as well as death of Leydig cells during the first wave of spermatogenesis (9), ischemia-induced neuronal death in a mouse ischemic stroke model (10, 11), gonadotropin-releasing hormone antagonist-induced death of testicular germ cells (12), ischemic death of myocytes (13), and oxidized LDL-induced death of vascular endothelial cells (14).

Humanin has other functions aside from inhibition of cell death. Humanin ameliorates cognitive impairment in wild-type mice caused by muscarinic receptor antagonists (15–17) or by intracerebroventricular injection of amyloid  $\beta$  (A $\beta$ ) (18–21), and cognitive impairment of aged familial AD-linked mutant gene-transgenic mice (22–24).

Since cognitive impairment in the aforementioned transgenic mouse model of AD is mainly caused by synaptic dysfunction of cholinergic neurons (25), it is highly likely that Humanin ameliorates synaptic dysfunction of cholinergic neurons. Humanin has also been shown to increase insulin sensitivity in the peripheral tissues via STAT3-mediated activation of the central nervous system (26) and preserve endothelial function and prevents atherosclerotic plaque progression in hypercholesterolemic apolipoprotein E-deficient mice (27).

Humanin elicits its activity by binding to its specific receptors (Ref. 28 for review). Bax was the first receptor of Humanin to be identified (29), and the binding of Humanin to intracellular Bax compromises the proapoptotic activity of Bax. Secreted Humanin binds to cell-surface formyl peptide receptor-like-1 and inhibits A $\beta$ -induced death of PC12 neuronal cells (30). Humanin also inhibits AD-related neuronal death via the heterotrimeric Humanin receptor (htHNR) on the cell membrane, which is composed of ciliary neurotrophic factor receptor  $\alpha$ ,

gen-activated protein kinase interaction motif; Sab, SH3 domain-binding protein that preferentially associates with Bruton's tyrosine kinase Btk; SH3BP5, SH3 domain-binding protein 5; SH3BD, SH3-binding domain.

## SH3BP5 Mediates Humanin Activity via JNK

WSX-1, and gp130 (31). The loss-of-function of any of the htHNR subunits abolishes Humanin-induced inhibition of AD-related neuronal death (31, 32). The binding of Humanin to htHNR results in oligomerization of the receptor subunits and the activation of JAK2 and STAT3 (22, 31–33), which is thought to alter expression of target genes of Humanin. However, it remains unknown which target genes of Humanin mediates the neuroprotective effect of Humanin.

SH3 domain-binding protein 5 (SH3BP5) was originally cloned as an interactor with Bruton's tyrosine kinase Btk (34) and alternatively named as Sab (SH3 domain-binding protein that preferentially associates with Btk). It was later cloned as an interactor with c-Jun NH<sub>2</sub>-terminal kinase (JNK) (35). SH3BP5 regulates Btk function in B lymphocytes negatively (36) and targets JNK to mitochondria where SH3BP5 may behave as a platform for the JNK-mediated signaling cascade (36).

In the current study, we found that Humanin increased SH3BP5 expression. Furthermore, overexpression of SH3BP5 inhibited AD-related cell death, while reduction of endogenous SH3BP5 expression attenuated the neuroprotective effect of Humanin. High levels of SH3BP5 directly inhibited JNK *in vitro*. These results indicate that SH3BP5 is an inhibitor of JNK and plays a substantial role as a transcriptional target and a downstream effector of Humanin.

### EXPERIMENTAL PROCEDURES

**Synthetic Peptides and Other Materials**—Humanin and S14G-Humanin (named Humanin G and abbreviated HNG; a Humanin analog with a 1000-fold stronger activity) (1, 2) were synthesized by the Keck Foundation Biotechnology Resource Laboratory of Yale University. Recombinant rat IL-6 was purchased from R&D Systems (Minneapolis). Rat CNTF was from PeproTech EC (London). A MitoTracker<sup>®</sup> was purchased from Invitrogen. A JAK2 inhibitor AG490 was purchased from Calbiochem.

**Differential Display**—Total RNA was prepared from human neuroblastoma SH-SY5Y cells, coincubated with 100 nM HNG for 3 h at 37 °C. The 1<sup>st</sup> strand cDNA was synthesized with Sensiscript RTase (Qiagen) using an oligo (dT)<sub>16</sub> as a primer. Double-stranded cDNAs were amplified with KOD polymerase (TOYOBO, Tokyo, Japan) using a random hexamer/oligo (dT)<sub>16</sub> primer mixture (Qiagen), and subjected to 7.5% acrylamide gel electrophoresis, and stained with ethidium bromide. cDNAs, the levels of which were increased by co-incubation with HNG, were dissected and eluted in distilled water. Eluted cDNAs were subcloned into TOPO vector (Invitrogen). The nucleotide sequences of the cDNAs were analyzed using an automated sequencer (ABI PRISM310 Genetic Analyzer, Applied Biosystems, PerkinElmer Life Sciences).

**Quantitative Real-time PCR Analysis**—Total RNA was extracted from cells using ISOGEN II (Nippon Gene). Reverse transcription and PCR were performed on an Applied Biosystems StepOnePlus<sup>™</sup> Real Time PCR System (Applied Biosystems) using the TaqMan RNA to CT 1-Step Kit (Applied Biosystems). The primer pairs and TaqMan probes for the target mRNAs were designed based on the human and mouse mRNA sequence using TaqMan Gene Expression Assays (Applied Biosystems, Assay ID: mouse GAPDH, Mm99999915\_g1; human

GAPDH, Hs99999905\_m1; mouse SH3BP5, Mm00449407\_m1; human SH3BP5, Hs00163137\_m1). Data analysis was performed using StepOne Software version 2.0.2 (Applied Biosystems). Data were normalized by level of mRNA expression of GAPDH.

**Genes and Vectors**—A London-type familial AD-linked amyloid  $\beta$  precursor protein (APP), V642I-APP, in the pcDNA3 vector (Invitrogen) was as described (1, 31). A human and mouse SH3BP5 cDNAs were PCR-amplified from total RNA of human neuroblastoma SH-SY5Y and neurohybrid F11 cells, respectively. For the generation of GST-human SH3BP5 (hSH3BP5) and 6 $\times$ His-mouse SH3BP5 (mSH3BP5) in bacteria, the human or mouse SH3BP5 cDNA was introduced into the pGEX-2T vector (GE Healthcare), which encodes a site for thrombin-mediated cleavage at the junction of GST and a transgene, and the pQE30 vector (Qiagen). The pQE30 vectors encoding 6 $\times$ His-mSH3BP5 deletion mutants and 6 $\times$ His-GST were similarly constructed. A recombinant protein generated by a pQE30 construct contains glycine between N-terminal 6 $\times$ His and a transgene-encoded protein and is detected by the antibody to HisG (Invitrogen). The cDNAs encoding human SH3BP5, mouse SH3BP5, and deletion mutants of mouse SH3BP5 were introduced into the pFLAG vector to generate C-terminally FLAG-tagged protein. pcDNA3-FLAG-human JNK-1a1 (100% identical to mouse JNK1a1) was purchased from Addgene. Constitutively active (ca) JNK and caASK1-encoding vectors were as described previously (37, 38). The mouse/rat (m/r) SH3BP5 cDNA was the mouse SH3BP5 cDNA in which three nucleotides of the mouse SH3BP5 siRNA-corresponding region were changed to the nucleotides of the rat SH3BP5 (A261T; A267G; A273G). All the other nucleotides of the mouse SH3BP5 siRNA-corresponding region of the rat SH3BP5 are equal to the mouse SH3BP5.

**siRNA Plasmids**—The siRNA vectors knocking down mouse and human SH3BP5 were constructed using the pRNA/U6.1-Shuttle vector or the pRNAT-U6.1-IRES-cGFP vector (GenScript) under the manufacturer's instruction (40). The sense and antisense DNA fragments of siRNAs were 5'-CGC-GGATCCCGCAAAGTACTATGTGCAGTTCAAGAGACTGCACATAGTACTTTGCCTTTTTTCCAAAAGCTTCCC-3' and 5'-GGGAAGCTTTTGAAAAAAGGCCAAAGTACTATGTGCAGTCTCTTGAAGTGCACATAGTACTTTGCCGGGATCCGCG-3', for human SH3BP5; 5'-CGC-GGATCCCGCTAGACGAAGTGGCAAAGATTCAAGAGATCTTTGCCAGTTCGTCTAGTTTTTTCCAAAAGCTTCCC-3' and 5'-GGGAAGCTTTTGAAAAAAGTGCAGTCTAGTGGCAAAGATCTCTTGAATCTTTGCCAGTTCGTCTAGCGGGATCCGCG-3' for mouse SH3BP5. These DNA fragments were annealed by heating and cooling according to the manufacturer's instructions, and inserted into the pRNA-U6.1-Shuttle vector and/or the pRNAT-U6.1-IRES-cGFP vector (GenScript).

**Immunocytochemistry and Immunohistochemistry**—Cells were fixed with 4% paraformaldehyde-PBS and sequentially immunostained with a primary antibody (SH3BP5 antibody) and a secondary antibody, Texas-red-conjugated, or fluorescein isothiocyanate (FITC)-conjugated goat anti-rabbit polyclonal antibody (Jackson ImmunoResearch Laboratories). Nuclei were

sometimes stained with DAPI (Sigma). The cells were observed with a confocal microscope LSM710 (Carl Zeiss). Some cells were transfected with an indicated vector or co-incubated with Humanin or HNG with/without a JAK2 inhibitor AG490 (Sigma Aldrich) before immunostaining. In some experiments, the SH3BP5 antibody was preabsorbed with an excess amount of the immunizing antigen GST-SH3BP5 or a negative control GST bound to glutathione-Sepharose beads to deplete SH3BP5-recognizing immunoglobulin.

All of the experimental procedures with mice were approved by the Institutional Animal Experiment Committees of Tokyo Medical University. Immunohistochemical analysis was performed as described previously (20). Mice were anesthetized, perfused transcardially with 100 mM sodium phosphate buffer (pH 7.4) and fixed with 100 mM sodium phosphate buffer (pH 7.4) containing 4% paraformaldehyde. Brains were embedded in frozen sections, and 10  $\mu$ m coronal sections were prepared on Matsunami adhesive silane-coated slides (MAS-GP; Matsunami Glass, Osaka, Japan). Samples were subsequently washed in PBS containing 0.1% Tween 20. Immunohistochemical detection was performed with the SH3BP5 antibody (1:50 dilution) and visualized with Tyramide-FITC method (TSA plus TMR/Fluorescein System; Perkin Elmer).

**Protein Analysis**—For the preparation of cell lysates, cells were washed twice with PBS, and suspended in 50 mM HEPES (pH 7.4), 150 mM NaCl, 0.1% Nonidet P-40, and protease inhibitor mixture Complete (Roche Diagnostics). After 2 $\times$  freeze-thaw, cell lysates were centrifuged at 15,000 rpm for 10 min at 4  $^{\circ}$ C, and the supernatants were subjected to immunoprecipitation, SDS-PAGE, and immunoblot analysis.

**Recombinant SH3BP5**—GST-SH3BP5 was expressed in *Escherichia coli* BL-21 at room temperature for 4 h in 1 mM isopropylthio- $\beta$ -D-galactopyranoside and purified using glutathione-Sepharose (GE Healthcare) according to the manufacturer's instructions. 6 $\times$ His-mSH3BP5, 6 $\times$ His-mSH3BP5 deletion mutants, and 6 $\times$ His-GST were expressed in *E. coli* M15[pREP4] (Qiagen) at 37  $^{\circ}$ C for 4 h in 1 mM isopropylthio- $\beta$ -D-galactopyranoside and purified with TALON metal resin (Clontech). Bound recombinant 6 $\times$ His proteins were washed with 10 mM imidazole solution and eluted with 250 mM imidazole solution according to the manufacturer's instructions. Eluted recombinant 6 $\times$ His proteins were desalted by Zeba Desalting Column (Pierce) and then one-tenth volume of 10 $\times$ PBS was added to the desalted protein solution. A considerable amount of non-specific proteins contaminated the recombinant 6 $\times$ His proteins purified with TALON Metal Resin. Therefore, mock purification was done using *E. coli* M15[pREP4] expressing the empty vector, and resulting contaminated proteins were used as a negative control of 6 $\times$ His-mSH3BP5. The concentration of purified recombinant proteins was determined using the BCA assay kit (Pierce).

**Antibodies**—The rabbit polyclonal antibody to human SH3BP5 was raised against the whole recombinant GST-hSH3BP5, produced in *E. coli*. Ready-made antibodies were purchased from following companies: anti-Myc and anti-HisG-HRP from Invitrogen; anti-FLAG (clone M2) from Sigma-Aldrich; anti-APP (clone 22C11) from Chemicon; anti-total JNK from Santa Cruz Biotechnology; anti-phospho-SAPK/JNK from

Cell Signaling Technology; anti-total JNK from Santa Cruz Biotechnology; anti-HA (clone 3F10) from Roche Diagnostics.

**Cells, Cell Death, and Cell Viability**—Neuronal cell death assays related to AD were first performed by Yamatsuji *et al.* (41) and previously described in detail (31). Human SH-SY5Y neuroblastoma cells, were grown in DMEM/Ham's F12 mixture (DMEM/F12) (Wako) containing 10% FBS, seeded at 2  $\times$  10<sup>5</sup>/well in six-well plates and incubated for 12–16 h, transfected with the appropriate vectors for 3 h in the absence of serum, and then cultured in DMEM/F12–10% FBS and/or Humanin or HNG. At 24 h after transfection, the media were replaced with DMEM/F12 containing N2 supplement (Invitrogen) and/or Humanin or its analog. At 48 h after the onset of transfection, cells were harvested for Trypan Blue cell death assays, cell viability assays using the WST-8 assay kit (Dojindo) and calcein AM (Dojindo), and their microscopic views were taken after staining with calcein AM to show viable cells that were attached to cell plates (31). F11 neurohybrid cells are described in earlier studies (1). F11 cells, seeded at 7  $\times$  10<sup>4</sup>/well in 6-well plates in Ham's F-12 plus 18% FBS and incubated for 12–16 h, were co-transfected with indicated vectors for 3 h in the absence of serum and then incubated with Ham's F-12 plus 18% FBS for 2 h. At 5 h after the onset of transfection, culture media were replaced by Ham's F-12 plus 10% FBS. At 24 h after transfection, the media were replaced by Ham's F-12 containing N2 supplement. At 72 h after the onset of transfection, the cells were harvested to perform microscopic analysis, Trypan Blue cell death assays, and WST-8 cell viability assays.

**Primary Hippocampal Neurons (PHNs) and Cell Death Assay**—Mouse PHNs were prepared from hippocampi of mouse E14 embryos, as shown in earlier studies (1, 32). They were seeded in poly-L-lysine-coated 6-well plates (Sumitomo Bakelite) at 5  $\times$  10<sup>5</sup> cells/well in Neuron medium (Sumitomo Bakelite). After incubation for 3 days (DIV3), the culture medium was replaced with DMEM containing N2 supplement. On DIV4, transfection was performed with Lipofectamine 2000 (Invitrogen), according to instructions. After transfection, Humanin or HNG was added to the media for co-incubation. At 48 h after transfection, cells were fixed with 4% paraformaldehyde for 30 min. Expression of V642I-APP and SH3BP5-FLAG was monitored by immunofluorescence analysis of these proteins in cells. The introduction of the siRNA-encoding vector into cells was monitored by immunofluorescence analysis of GFP in cells. Apoptosis of PHNs was determined by morphological examination of nuclei stained with DAPI, as described in our earlier study (42).

**In Vitro Binding Assays**—FLAG-JNK-1a1 was overexpressed in F11 cells by transfection. FLAG-JNK-1a1, immunoprecipitated from cell lysates with the FLAG antibody, was mixed with recombinant 6 $\times$ His-GST, 6 $\times$ His-mSH3BP5, or a 6 $\times$ His-mSH3BP5 deletion mutant, incubated at 4  $^{\circ}$ C overnight, washed extensively, and subjected to SDS-PAGE and immunoblot analysis.

**In Vitro JNK Kinase Assays**—F11 cells, transfected with the pcDNA3-FLAG-JNK-1a1, were coincubated with 10  $\mu$ M anisomycin for 3 h, and the lysates were prepared from these cells. Other lysates were prepared from F11 cells and transfected with the empty vector or the vector encoding human SH3BP5.

## SH3BP5 Mediates Humanin Activity via JNK

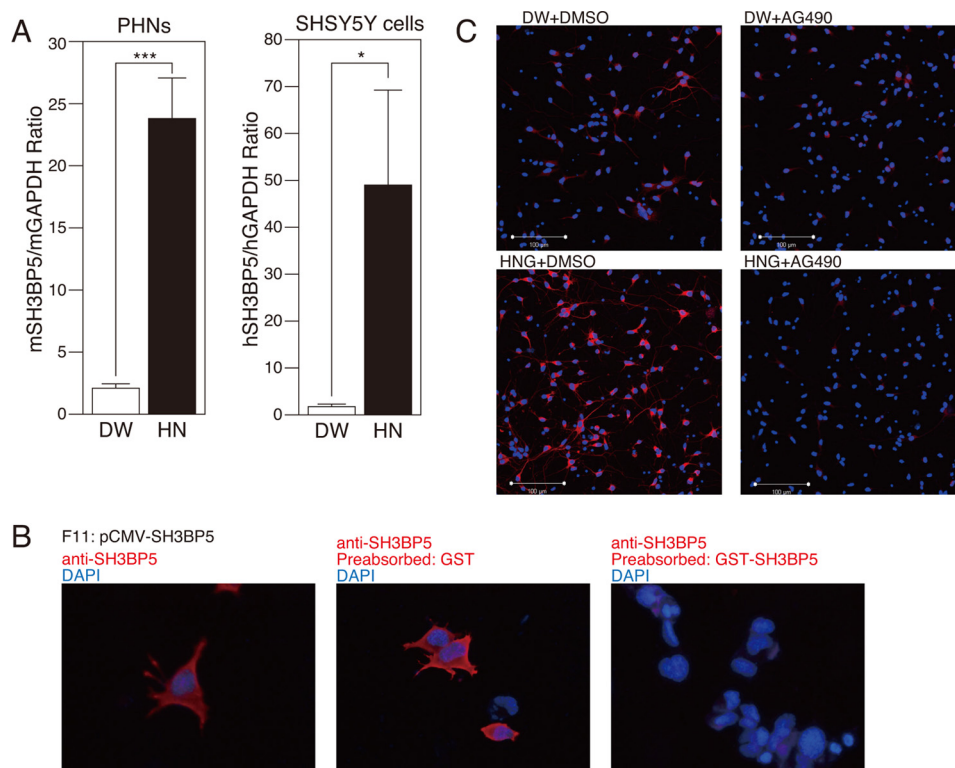


**FIGURE 1. Both mRNA and protein expressions of SH3BP5 are induced by Humanin.** *A*, real-time PCR analysis of SH3BP5 and GAPDH mRNAs, prepared from mouse PHNs and human SH-SY5Y cells, incubated with 10  $\mu$ M HN or distilled water (DW) for 24 h. This experiment was performed with  $n = 3$ ; \*\*\*,  $p < 0.001$ ; \*,  $p < 0.05$ . *B*, F11 cells, transfected with the pCMV-human SH3BP5 vector, were immunostained with the SH3BP5 antibody (red), not preabsorbed (left), preabsorbed with GST (middle), or preabsorbed with GST-SH3BP5 (right), which had been immobilized onto glutathione-Sepharose, for 24 h. Nuclei were stained with DAPI (blue). *C*, immunocytochemical analysis of SH-SY5Y cells with the SH3BP5 antibody (red), incubated with 100 nM Humanin G (HNG) or distilled water (DW) in the presence or the absence of 5  $\mu$ M AG490 for 24 h. Nuclei were stained with DAPI (blue).

FLAG-tagged JNK-1a1-containing lysates were then mixed with the lysates containing or not containing exogenously expressed SH3BP5 and incubated at 4 °C for 4 h. Then, FLAG-JNK-1a1 in the mixed lysates was immunoprecipitated with the FLAG antibody (M2), and immunoprecipitates were used for *in vitro* JNK kinase assay using a recombinant c-Jun protein as a substrate (KinaseSTAR JNK Activity Assay Kit, BioVision Research Products). Supernatants of *in vitro* JNK kinase assays were fractionated with SDS-PAGE, and the amount of phosphorylated c-Jun (phospho c-Jun) was analyzed by immunoblot analysis with antibodies to phospho c-Jun. Amounts of FLAG-JNK-1a1 and human SH3BP5 bound to the beads were similarly examined by immunoblot analysis with the antibodies to FLAG and SH3BP5.

In some experiments, FLAG-JNK-1a1, immunoprecipitated from the lysates, was mixed with a defined amount of recombinant 6 $\times$ His-mSH3BP5 (and/or its negative control), purified from bacteria, and a recombinant c-Jun protein as a substrate (BioVision), and incubated at 30 °C for 4 h. The whole reaction mixtures (30  $\mu$ l) containing beads were then mixed with the 1/3 volume of the 3 $\times$  SDS-PAGE sample buffer and subjected to SDS-PAGE and immunoblot analysis with the antibody to phospho c-Jun, the FLAG antibody (M2) for the detection of FLAG-JNK-1a1, and the HisG-HRP antibody for the detection of 6 $\times$ His-mSH3BP5.

**Statistical Analysis**—All cell death experiments were performed with  $n = 3$ . All values in figures are means  $\pm$  S.D. Statistical analysis was performed using one-way analysis of variance, followed by Bonferroni/Dunn post hoc analysis. All data were

analyzed using StatView (version 5.0.1) software from SAS Institute (Cary) (\*\*\*,  $p < 0.001$ ; \*\*,  $p < 0.01$ ; \*,  $p < 0.05$ ; n.s., not significant).

## RESULTS

**SH3BP5 Is a Transcriptional Target of Humanin**—To search for transcriptional targets of Humanin, a RT-PCR-assisted differential display screening was performed using mRNA from SH-SY5Y neuroblastoma cells that had been incubated with Humanin. We identified several genes, including SH3BP5, whose mRNA levels were increased by treatment with Humanin. In the current study, we investigated whether SH3BP5 mediates the neuroprotective effect of Humanin.

Using a quantitative PCR analysis, we confirmed that mRNA expression of SH3BP5 was up-regulated by approximately 10-fold by treatment with Humanin in both primary mouse hippocampal neurons (PHNs) and SH-SY5Y cultured human neuroblastoma cells (Fig. 1A).

Immunocytochemical analysis of F11 cells transfected with human SH3BP5 revealed SH3BP5 immunoreactivity. This was absent when the SH3BP5 antibody was preincubated with immunizing antigen GST-SH3BP5 (right panel), but not with GST (middle panel) (Fig. 1B), indicating that the antibody specifically recognized SH3BP5. Immunocytochemical analysis of SH3BP5 showed that incubation with a Humanin analog S14G-Humanin (named Humanin G; abbreviated HNG) (100 nM) increased SH3BP5 expression in SH-SY5Y cells (Fig. 1C). The effect of Humanin is mediated by a JAK2 and STAT3-mediated

signaling pathway, which is triggered by the binding of Humanin to the htHNR (31). In agreement with this notion, addition of AG490, a specific JAK2 inhibitor, to the incubation media nullified the HNG-induced increase in SH3BP5 expression (Fig. 1C).

**SH3BP5 Is Expressed Ubiquitously in Neuronal Tissues**—Immunohistochemical analysis was performed to examine the endogenous expression of SH3BP5 in neuronal tissues. Although SH3BP5 was ubiquitously expressed in neuronal cells including mouse hippocampal and cortical neurons, the level of SH3BP5 expression among neurons was not uniform. The level of SH3BP5 expression was high in the neurons of the CA3 region of hippocampus, pons, and hypothalamus, whereas it was low in the neurons of cortex, dentate gyrus of hippocampus, and cerebellum (Fig. 2A). By doubly staining F11 cells with the SH3BP5 antibody and Mitotracker®, a mitochondrial marker, we confirmed that SH3BP5 was colocalized with mitochondria (Fig. 2B), as shown in a previous study (39).

**Overexpression of SH3BP5 Inhibits V642I-APP-induced Neuronal Death**—Based on the finding that SH3BP5 is a transcriptional target of Humanin, we hypothesized that SH3BP5 mediates the neuroprotective effect of Humanin. Exogenous expression of V642I-APP, a London-type familial AD-linked gene, causes death of certain types of cultured neuronal cells (Refs. 43, 44 for review). Using this *in vitro* model, we examined the effect of overexpression of SH3BP5 on V642I-APP-induced neuronal death. Reproducibly, exogenous expression of V642I-APP induced death of F11 neurohybrid cells (Fig. 3, A–D). Coexpression of SH3BP5 with V642I-APP attenuated V642I-APP-induced death (Fig. 3, A–D), and this effect was recapitulated in PHNs (Fig. 3E) and SH-SY5Y cells (Fig. 4).

**Reduction of Endogenous SH3BP5 Expression Attenuates the Neuroprotective Effect of Humanin**—We next asked whether SH3BP5 is essential for Humanin-mediated neuroprotection. To this end, plasmid-based siRNAs (40) for human and mouse SH3BP5 were constructed, and their silencing effects were tested. Cotransfection of a vector encoding a siRNA for human SH3BP5 with a vector encoding human SH3BP5 attenuated the level of human SH3BP5 expression (Fig. 5A). Similarly, co-expression of a siRNA for mouse SH3BP5 with a vector encoding mouse or rat/mouse SH3BP5 (see “Experimental Procedures”) attenuated the level of mouse or rat/mouse SH3BP5 (Fig. 5A).

As shown previously (1), incubation with 10  $\mu$ M Humanin reproducibly inhibited the V642I-APP-induced death of F11 cells (Fig. 5, B–D). Coexpression of the siRNA for mouse SH3BP5 with V642I-APP attenuated the Humanin-induced inhibition of the V642I-APP-induced death of F11 cells (Fig. 5, B–D). Similarly, coexpression of the siRNA for human and mouse SH3BP5 attenuated the Humanin-induced inhibition of V642I-APP-induced death of SH-SY5Y cells (Fig. 6, A–C) and PHNs (Fig. 6D), respectively. These results indicate that SH3BP5 is required for the Humanin-mediated neuroprotective effect in these cells.

**Overexpression of SH3BP5 Inhibits Neuronal Death Induced by Constitutively Active ASK1 (caASK1) and caJNK**—V642I-APP-induced death is intracellularly mediated by apoptosis signal-stimulating kinase-1 (ASK1) and JNK (37, 38, 43, 44). Given that Humanin also inhibits caASK1- and caJNK-triggered neuronal cell death (37, 38), we first examined whether expression of

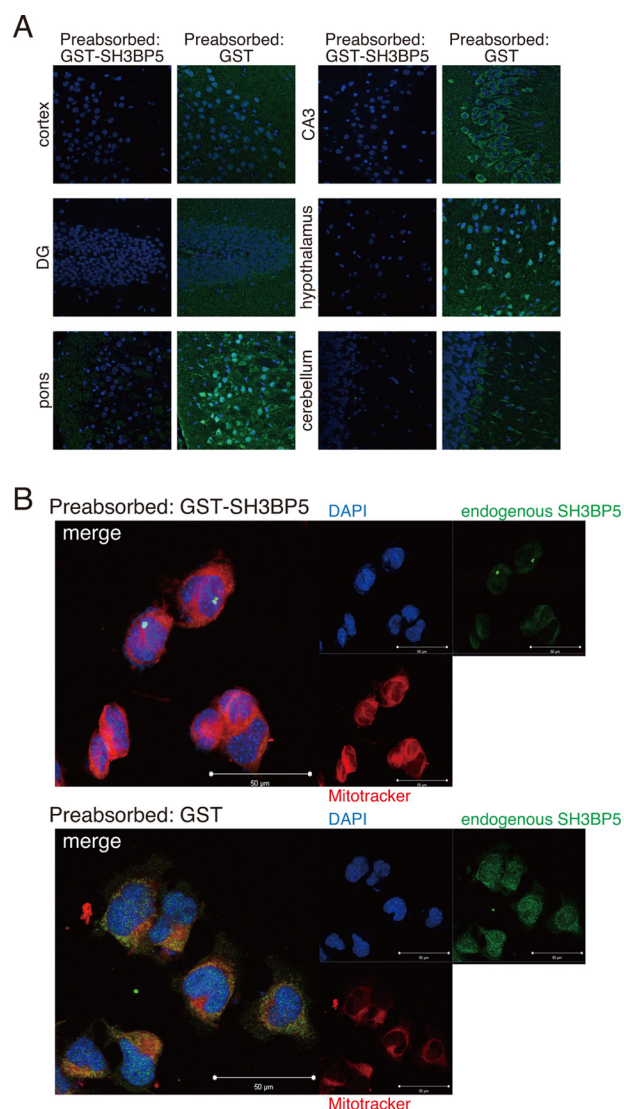


**FIGURE 2. SH3BP5 is ubiquitously expressed and localized in mitochondria.** A, immunohistochemical analysis of SH3BP5 expression in various mouse neuronal tissues using the SH3BP5 antibody (green). The SH3BP5 antibody was preincubated (preabsorbed) with GST (a negative control) or GST-SH3BP5 (immunizing protein), bound to glutathione-Sepharose, for 24 h. Nuclei were stained with DAPI (blue). B, F11 cells were immunostained with the SH3BP5 antibody (green) and the MitoTracker® (red). Nuclei were stained with DAPI (blue). The SH3BP5 antibody was preincubated (preabsorbed) with GST (a negative control) or GST-SH3BP5 (immunizing protein), bound to glutathione-Sepharose, for 24 h. Nuclei were stained with DAPI (blue).

SH3BP5 prevents this cell death. Both caASK1- and caJNK-elicited cell deaths were inhibited by overexpression of SH3BP5 (Fig. 7, A and B). This result indicates that at least one target of SH3BP5 is JNK itself or its downstream molecule.

**SH3BP5 Is a Direct Inhibitor of JNK**—We next hypothesized that SH3BP5 directly interferes with JNK. To test this, we performed two independent *in vitro* reconstitution JNK assays. Cell lysates from F11 cells overexpressing FLAG-JNK-1a1 and SH3BP5 were combined, and then FLAG-JNK-1a1 was immunoprecipitated. *In vitro* JNK assays were performed using the FLAG-JNK-1a1 immunoprecipitates and recombinant c-Jun protein as a JNK substrate. SH3BP5 bound to JNK and inhibited JNK activity in a SH3BP5 dose-responsive fashion (Fig. 8A).

## SH3BP5 Mediates Humanin Activity via JNK

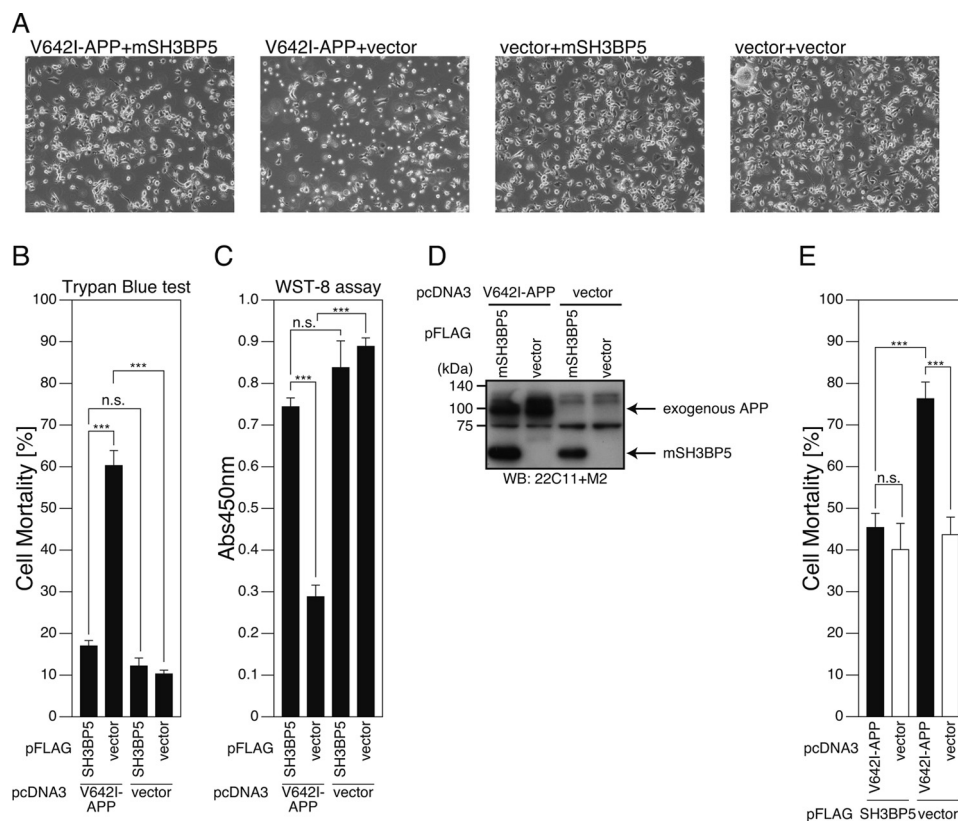


**FIGURE 3. Overexpression of SH3BP5 inhibits V642I-APP-induced death of mouse neuronal cells.** A–D, F11 cells were cotransfected with the empty pFLAG vector (*vector*) or the pFLAG vector encoding mouse SH3BP5 (mSH3BP5) together with the empty pcDNA3 vector (*vector*) or pcDNA3-V642I-APP (V642I-APP). At 72 h after transfection, they were harvested for microscopic analysis (A), Trypan Blue cell death assays (B), and WST-8 cell viability assays (C). Cell lysates were subjected to SDS-PAGE and immunoblot analysis with FLAG antibody (M2) and APP antibody (22C11) (D). E, PHNs were cotransfected with the empty pFLAG vector (*vector*) or the pFLAG vector encoding mSH3BP5 together with the empty pcDNA3 vector (*vector*) or pcDNA3-V642I-APP (V642I-APP). At 48 h after transfection, the cells were immunostained with both the APP and FLAG antibodies. Nuclei were stained with DAPI. For the calculation of cell-death percentages in the cells that had been transfected with the two empty vectors, the percentages of morphologically apoptotic cells in total cells were counted. For the calculation of cell-death percentages in the cells that had been cotransfected with the empty vector and the V642I-APP-encoding vector, with the mSH3BP5-encoding vector and the empty vector, or with the V642I-APP- and mSH3BP5-FLAG-encoding vectors, the percentages of apoptotic cells in the cells that overexpressed V642I-APP, SH3BP5-FLAG, and both V642I-APP and mouse SH3BP5-FLAG, were counted, respectively. This study was performed with  $n = 3$ ; 50–100 cells were counted per well. \*\*\*,  $p < 0.001$ ; n.s., not significant.

We also examined whether purified recombinant SH3BP5 N-terminally tagged with 6×His (H6-SH3BP5), produced in bacteria, interferes JNK activity *in vitro*. To this end, we mixed FLAG-JNK-1a1, which was immunoprecipitated from F11 cells, with varying amounts of H6-SH3BP5 and performed *in vitro* JNK assays. H6-SH3BP5 inhibited JNK activity in a dose-dependent fashion (Fig. 8B).

**SH3BP5 Mediates the Humanin-induced Inhibition of JNK Phosphorylation, Caused by Exogenous Expression of V642I-APP**—We next examined whether Humanin affected the phosphorylation of JNK. In accordance with the finding that the V642I-APP-induced death is mediated by a signaling pathway that involves JNK (37, 38, 43, 44), exogenous expression of V642I-APP increased the level of phosphorylated JNK (p-JNK) (Fig. 8C, lane 5). Furthermore, the increase in the level of p-JNK was reduced by treatment with 10  $\mu\text{M}$  Humanin (Fig. 8C, lane 6). Importantly, we found that siRNA-mediated reduction of endogenous SH3BP5 expression abolished the Humanin-induced reduction of p-JNK (Fig. 8C, lanes 7 and 8). This finding indicates that SH3BP5 is essential for the Humanin-induced inhibition of the phosphorylation of JNK caused by exogenous expression of V642I-APP.

**Both KIM 1 and 2 of SH3BP5 Are Involved in Inhibiting JNK Activity**—SH3BP5 contains an SH3-binding domain (SH3BD) and two putative mitogen-activated protein kinase interaction motifs (KIMs) named KIM1 and KIM2 (Fig. 9A) (35, 39). To identify domain(s) of mouse SH3BP5 that are involved in functionally interacting with JNK, we produced a recombinant N-terminally 6×His-tagged mouse SH3BP5 protein that lacks SH3BD, KIM1, KIM2, KIM1 plus KIM2, or SH3BD plus KIM1 plus KIM2, in bacteria (Fig. 9A). Deletion of KIM1 and/or KIM2 did not increase but rather slightly decreased the migrating distance from the origin in SDS-PAGE for unknown reasons (Fig. 9, B and C, compare full-length SH3BP5 with SH3BP5 lacking KIM1, KIM2, or KIM1 plus KIM2). *In vitro* binding assays showed that SH3BP5 lacking SH3BD plus KIM1 plus KIM2 did not bind to JNK, while any other deletion mutant did (Fig. 9D). This result suggests that SH3BP5 binds to JNK through SH3BD, KIM1, and KIM2. On the other hand, *in vitro* JNK kinase assays revealed that SH3BP5 lacking KIM1 plus KIM2 or SH3BP5 lacking SH3BD plus KIM1 plus KIM2 did not inhibit the JNK kinase activity, while any other deletion mutant did (Fig. 10A). In accordance with the latter result, overexpression of C-terminally FLAG-tagged SH3BP5 lacking KIM1 plus KIM2 or

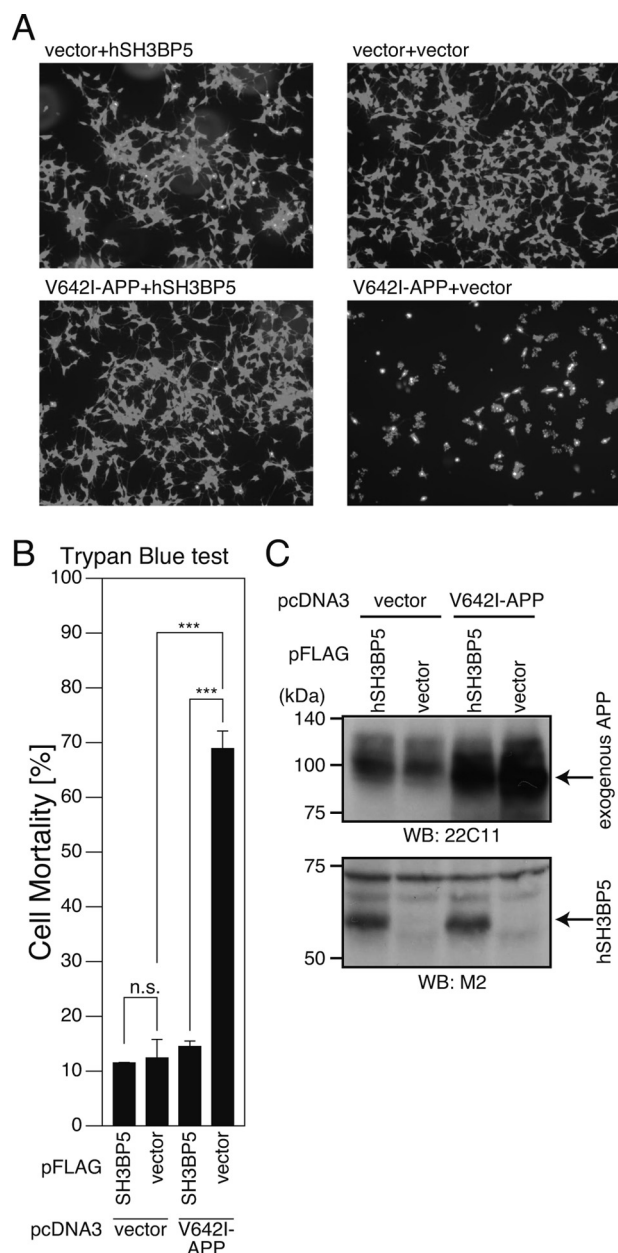


**FIGURE 4. Overexpression of human SH3BP5 inhibits V642I-APP-induced death of SH-SY5Y cells.** SH-SY5Y cells, cotransfected with the empty pFLAG vector (*vector*) or the pFLAG vector encoding human SH3BP5 (*hSH3BP5*) together with the empty pcDNA3 vector (*vector*) or pcDNA3-V642I-APP (V642I-APP). At 48 h after transfection, they were harvested for microscopic analysis after staining with calcein (A) and Trypan Blue cell death assays (B). Cell lysates were subjected to SDS-PAGE and immunoblot analysis with M2 antibody to FLAG and APP antibody (22C11) (C). \*\*\*,  $p < 0.001$ ; *n.s.*, not significant.

SH3BP5 lacking SH3BD plus KIM1 plus KIM2 did not inhibit V642I-APP-induced death of SH-SY5Y cells, while any other deletion mutant did (Fig. 10B). These results indicate that deletion of both KIM1 and KIM2 is necessary to disrupt the JNK-inhibiting activity of SH3BP5 and that both KIM1 and KIM2 of SH3BP5 are independently involved in inhibiting JNK.

## DISCUSSION

JNK promotes apoptosis through two pathways: the first pathway is mediated by JNK-induced phosphorylation and transacti-

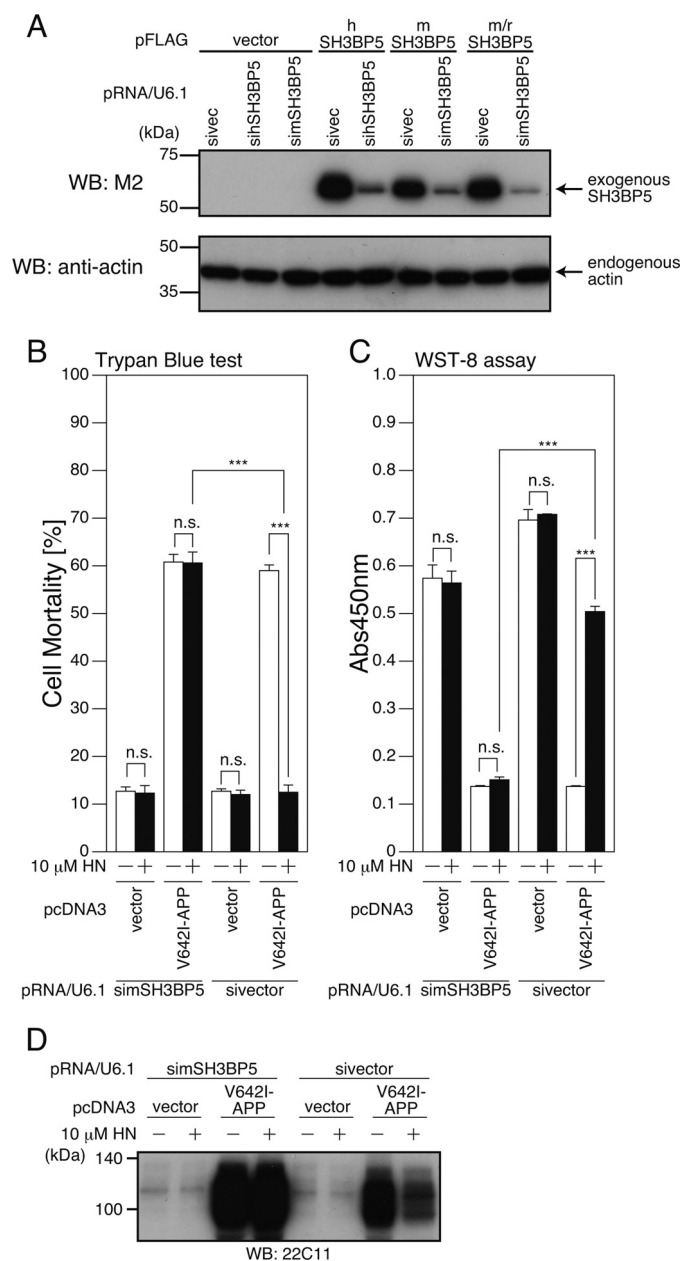


**FIGURE 5. siRNA-mediated reduction of endogenous SH3BP5 expression inhibits the neuroprotective effect of Humanin in F11 neurohybrid cells.**

A, F11 cells were transfected with the empty pFLAG vector (*vector*) or the pFLAG vector encoding human SH3BP5 (*hSH3BP5*), mouse SH3BP5 (*mSH3BP5*), or mouse SH3BP5 in which three nucleotides in the mouse SH3BP5 siRNA corresponding region were changed to the nucleotides of the rat SH3BP5 (*m/rSH3BP5*), together with the pRNA-U6.1-Shuttle vector (*sivector*) or the pRNA-U6.1-Shuttle vector encoding siRNA for human and mouse SH3BP5 (*sihSH3BP5* and *simSH3BP5*). At 72 h after transfection, cell lysates were subjected to SDS-PAGE and immunoblot analysis with antibodies to FLAG (M2) and actin. B–D, F11 cells were cotransfected with the empty pcDNA3 vector (*vector*) or pcDNA3-V642I-APP (V642I-APP) together with the pRNA-U6.1-Shuttle vector (*sivector*) or the pRNA-U6.1-Shuttle vector encoding siRNA for mouse SH3BP5 (*simSH3BP5*) in the presence or the absence of 10  $\mu$ M HN. At 72 h after transfection, they were harvested for Trypan Blue cell death assays (B), and WST-8 cell viability assays (C). Cell lysates were subjected to SDS-PAGE and immunoblot analysis with the APP antibody (22C11) (D). \*\*\*,  $p < 0.001$ ; *n.s.*, not significant.

vation of multiple transcription factors such as c-Jun and ATF2, which up-regulate the expression of proapoptotic genes and down-regulate anti-apoptotic genes; and the second pathway,

## SH3BP5 Mediates Humanin Activity via JNK

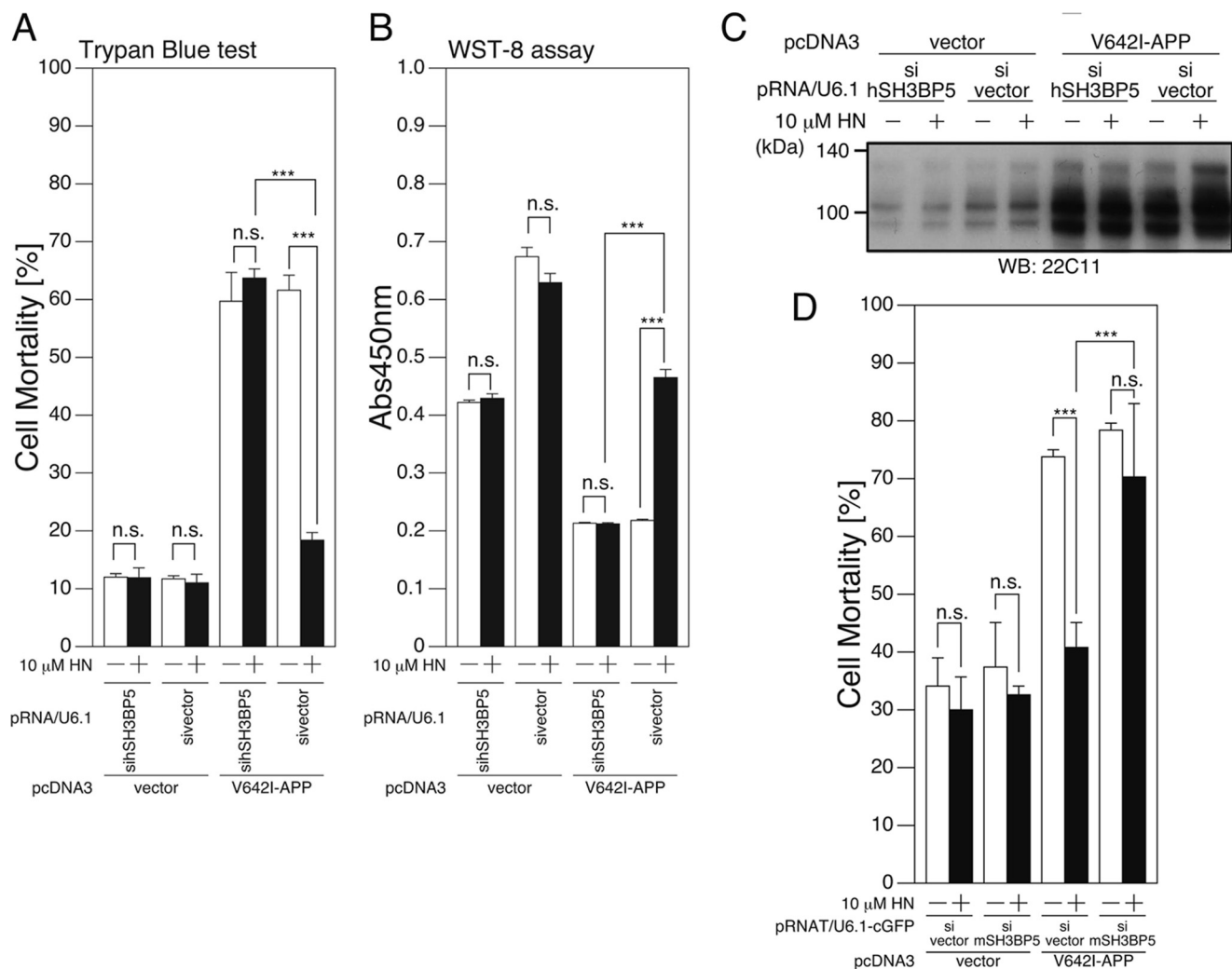


**FIGURE 6. siRNA-mediated reduction of SH3BP5 attenuates the neuroprotective effect of Humanin in human SH-SY5Y cells and mouse primary hippocampal neurons.** A–C, SH-SY5Y cells, cotransfected with the empty pcDNA3 vector (*vector*) or pcDNA3-V642I-APP (V642I-APP) together with the pRNA/U6.1-Shuttle vector (*sivector*) or the pRNA/U6.1-Shuttle vector encoding siRNA for human SH3BP5 (sihSH3BP5) in the presence or the absence of 10  $\mu$ M HN. At 48 h after transfection, they were harvested for Trypan Blue cell death assays (A) and WST-8 cell viability assays (B). Cell lysates were subjected to SDS-PAGE and immunoblot analysis with the APP antibody (22C11) (C). D, PHNs were cotransfected with the empty pcDNA3 vector (*vector*) or pcDNA3-V642I-APP (V642I-APP) together with the pRNAT-U6.1-IRES-cGFP vector (*sivector*) or the pRNAT-U6.1-IRES-cGFP encoding siRNA for mouse SH3BP5 (simSH3BP5). At 48 h after transfection, the cells were stained with the APP antibody. cGFP was expressed in cells into which the *sivector* or the simSH3BP5-encoding vector had been introduced. Nuclei were stained with DAPI. The percentages of morphologically apoptotic cells in the cells that expressed both V642I-APP plus cGFP were counted for the pcDNA3-V642I-APP-transfected cells. The percentages of apoptotic cells in the cells that expressed cGFP were counted for the pcDNA3 vector-transfected cells. This study was performed with  $n = 3$ ; 50–100 cells were counted per well. \*\*\*,  $p < 0.001$ ; n.s., not significant.

which is mediated by JNK-induced phosphorylation and modulation of proapoptotic and anti-apoptotic proteins in the mitochondria (45). SH3BP5 targets JNK to mitochondria (39), which is a function that is essential for the activation of mitochondrial JNK and the occurrence of a certain types of cell death. In support of this, the blockade of the binding of SH3BP5 to JNK by a peptide mimic of the Sab kinase-interacting motif-1 (46) or the shRNA-mediated reduction of endogenous SH3BP5 expression leads not only to a reduction in the activation of mitochondrial JNK, but also the inhibition of acetaminofen- and TNF $\alpha$ -induced hepatotoxicity (47), the 6-hydroxydopamine-induced toxicity (48), and ischemia/reperfusion injury in cardiomyocytes (49).

V642I-APP-induced neuronal death is mediated by APP, Go, Rac1 (or Cdc42), ASK1, JNK, NADPH oxidase, and caspases in order of activation (37, 38, 43, 44). NADPH oxidases, contain-

ing six transmembrane domains, localize in the plasma membrane and other intracellular membranes (50) and play a central role in the synthesis of reactive oxygen species in the non-mitochondrial cytoplasm. The essential role of NADPH oxidases in V642I-APP-induced death suggests that cytoplasmic JNK, but not mitochondrial JNK, may mediate this signal. Consistent with this, the siRNA-mediated reduction of endogenous SH3BP5 expression, which inhibited the SH3BP5-mediated targeting of JNK to mitochondria, did not impair V642I-APP-induced death (Fig. 5, B and C).

By performing *in vitro* reconstitution JNK assays, the present study demonstrated that SH3BP5 directly inhibits JNK in a dose-responsive fashion *in vitro* (Fig. 8, A and B). Considering this result and the published data indicating that the endogenous level of SH3BP5 targets JNK to mitochondria and thereby positively regulates JNK (47–49), we postulate that when the



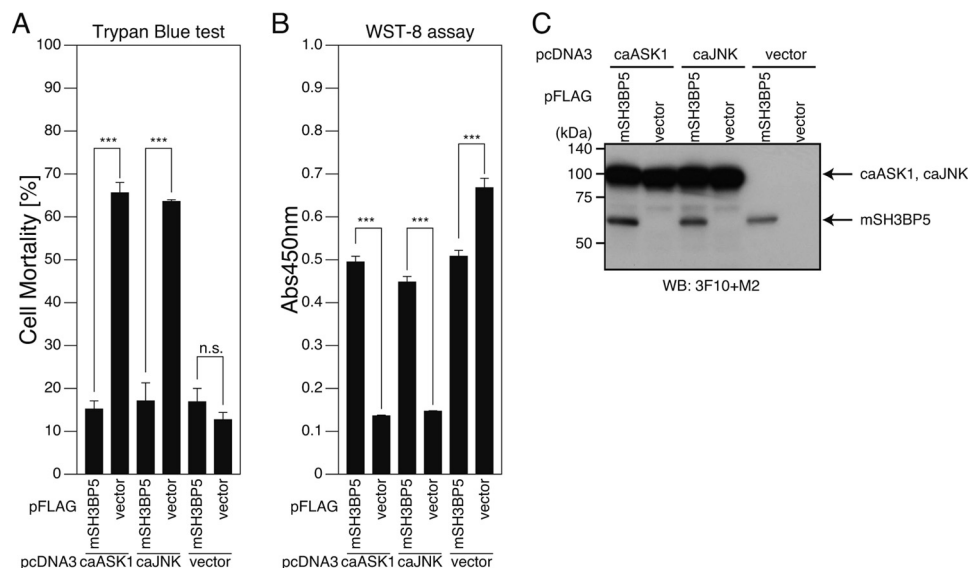


FIGURE 7. **SH3BP5 inhibits constitutive active ASK1- and JNK-induced proapoptotic pathways.** A–C, F11 cells were cotransfected with the empty pcDNA3 vector (*vector*), pcDNA3-constitutive active (*ca*)ASK1 or pcDNA3-*ca*JNK together with the empty pFLAG vector (*vector*) or the pFLAG vector encoding mouse SH3BP5 (mSH3BP5). At 72 h after transfection, they were harvested for Trypan Blue cell death assays (A) and WST-8 cell viability assays (B). Cell lysates were subjected to SDS-PAGE and immunoblot analysis with the FLAG antibody (M2) (for the detection of mSH3BP5-FLAG) and the monoclonal HA antibody (3F10) (for the detection of HA-tagged *ca*ASK1 and *ca*JNK) (C). \*\*\*,  $p < 0.001$ ; *n.s.*, not significant.

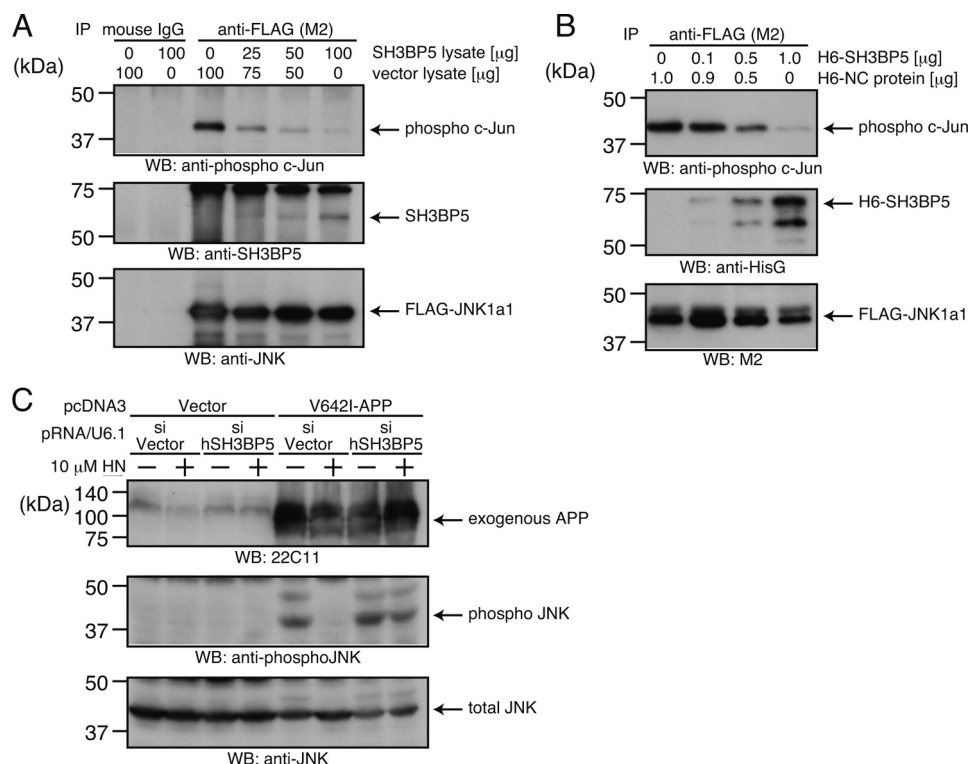
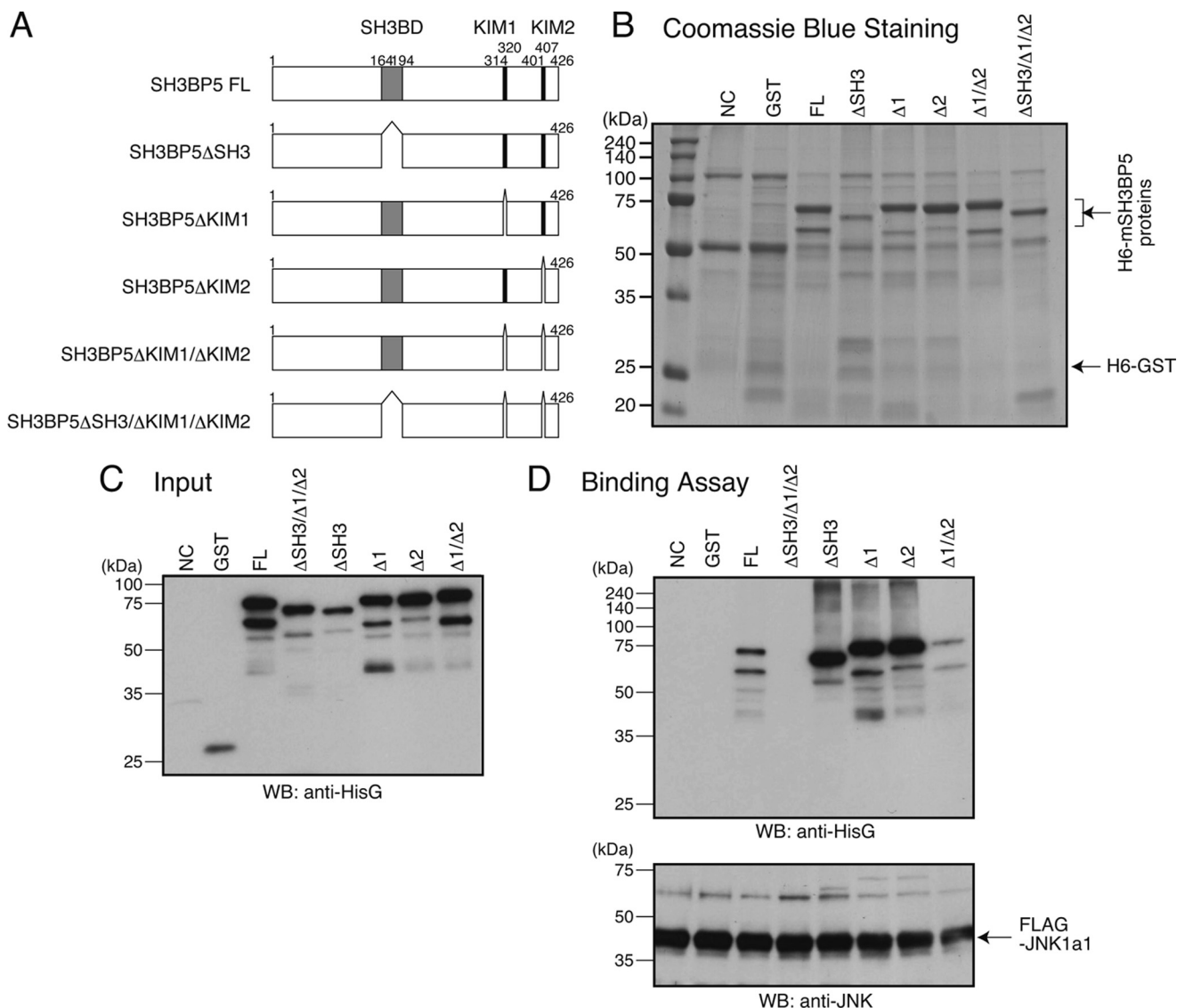


FIGURE 8. **SH3BP5 inhibits JNK and mediates the Humanin-induced inhibition of JNK phosphorylation.** A, lysates (100 μg) of the FLAG-JNK-1a1-overexpressing F11 cells, treated with 10 μM anisomycin (to activate the JNK pathway), were mixed with indicated amounts of lysates of the mouse SH3BP5-overexpressing and/or the empty vector-transfected F11 cells. Lysates of empty vector-transfected cells were added to make the total amounts of lysates equal (200 μg). FLAG-JNK-1a1 in the mixed lysates was immunoprecipitated with the FLAG (M2) antibody or mouse IgG (negative control) and subjected to *in vitro* JNK kinase assays using recombinant c-Jun as a substrate. JNK activity was monitored by the detection of phospho c-Jun in the supernatants. Amounts of co-precipitated SH3BP5 and FLAG-JNK-1a1 on the beads were also monitored by SDS-PAGE and immunoblot analysis with the SH3BP5 and JNK antibodies. B, FLAG-JNK-1a1, immunoprecipitated from the cell lysates with the FLAG antibody, was mixed with indicated amounts of recombinant 6×His-mSH3BP5 (H6-SH3BP5) and subjected to *in vitro* JNK kinase assays using recombinant c-Jun as a substrate. Appropriate amounts of the negative control protein (H6-NC), purified from bacteria expressing the control vector, were added to make the total amount of the recombinant proteins equal. The whole reaction mixtures were then subjected to SDS-PAGE and immunoblot analysis with the antibody to phospho c-Jun, the antibody to HisG for the detection of 6×His-mSH3BP5, and the antibody to FLAG for the detection of FLAG-JNK-1a1. C, SH-SY5Y cells were cotransfected with the empty pcDNA3 vector (*vector*) or pcDNA3-V642I-APP (V642I-APP) together with the pRNA/U6.1-Shuttle vector (*si*vector) or the pRNA/U6.1-Shuttle vector encoding siRNA for human SH3BP5 (*si*hSH3BP5). Humanin (HN) was added to the culture medium (10 μM) just after the end of transfection. At 72 h after the start of transfection, the cells were harvested for SDS-PAGE and immunoblot analysis with indicated antibodies.

## SH3BP5 Mediates Humanin Activity via JNK



**FIGURE 9. SH3BP5 binds to JNK through SH3BD, KIM1, and KIM2.** *A*, structure of mouse SH3BP5 (mSH3BP5) and deletion mutants of mSH3BP5. *B*, 6 $\times$ His-mSH3BP5 (H6-mSH3BP5) or its deletion mutant, produced in bacteria, was purified with TALON Metal Resin. Negative-control purification (NC) was equally done from bacteria in which the empty vector was introduced. The purified proteins were fractionated by SDS-PAGE, followed by Coomassie Blue staining. *FL*: SH3BP5 full-length,  $\Delta$ SH3: SH3BP5 lacking SH3BD,  $\Delta$ 1: SH3BP5 lacking KIM1,  $\Delta$ 2: SH3BP5 lacking KIM2. *C*, 6 $\times$ His-GST, 6 $\times$ His-mSH3BP5, and 6 $\times$ His-mSH3BP5 deletion mutants were produced in bacteria and purified with TALON Metal Resin. Each protein (0.1  $\mu$ g) was fractionated as an input for SDS-PAGE and subjected to immunoblot analysis with antibody to HisG. *D*, FLAG-JNK-1a1, immunoprecipitated from the cell lysates with the FLAG antibody, was mixed with indicated recombinant 6 $\times$ His-GST, 6 $\times$ His-mSH3BP5, or a 6 $\times$ His-mSH3BP5 deletion mutant (1  $\mu$ g per sample), washed extensively, and subjected to SDS-PAGE and immunoblot analysis. Immunoblot analysis was performed with the antibody to HisG for the detection of 6 $\times$ His-tagged recombinant proteins and the M2 antibody to FLAG for the detection of FLAG-JNK-1a1.

molar ratio of SH3BP5 to JNK in the SH3BP5/JNK complex is below a certain threshold level, SH3BP5 only functions as a carrier of JNK to mitochondria. When the molar ratio exceeds this threshold level, SH3BP5 inhibits JNK.

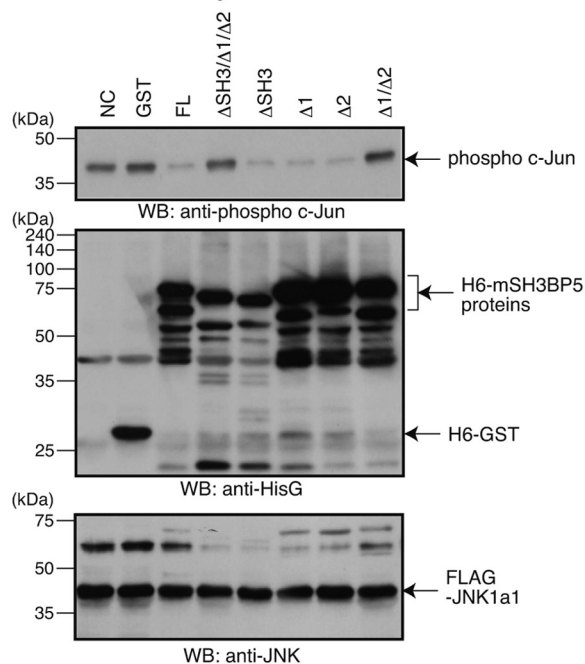
JNK-interacting protein-1 (JIP-1) was originally identified as an inhibitor of JNK (51). *In vitro* reconstitution assays show that recombinant JIP-1 directly inhibits JNK by competing with the substrates of JNK for binding to JNK. In addition, overexpression of JIP-1 retained JNK in the cytoplasm. Through these two mechanisms, JIP-1 inhibits the JNK-mediated phosphorylation of its substrates (51). In agreement, overexpression of JIP-1 suppressed the effects of the JNK signaling pathway on cellular proliferation, including transformation by the Bcr-Abl oncogene (51). However, the subsequent investigation

on JIP-1 has established that JIP-1 is an essential scaffold protein for MAP kinase cascade consisting of mixed-lineage kinases (or dual leucine zipper kinases), MKK7/MKK4, and JNK (52).

Importantly, as a scaffold protein, JIP-1 positively regulates the progression of this signal transduction cascade (52). These findings suggest that, similar to SH3BP5, JIP-1 may behave an inhibitor of JNK only when its overexpression magnitude exceeds a certain threshold level, although the detailed mechanism underlying this functional alteration remains undefined.

SH3BP5 may have targets aside from JNK. In the current study, the siRNA-mediated reduction of endogenous SH3BP5 expression attenuated the Humanin-mediated suppression of the V642I-APP-induced increase in the phosphorylation of

## A Kinase Assay



## B Trypan Blue Test

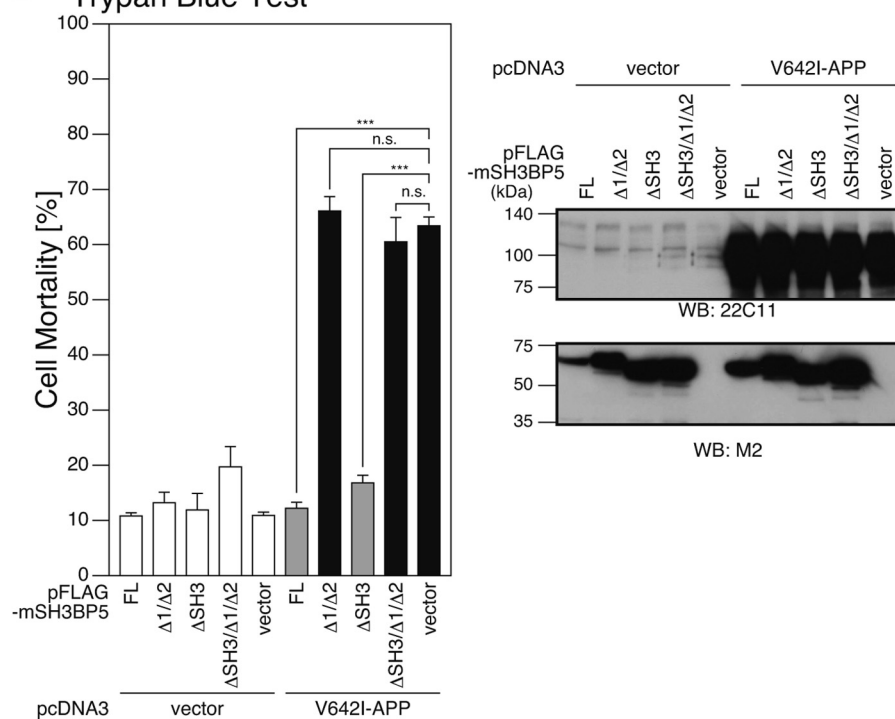


FIGURE 10. **Both KIM1 and KIM2 of SH3BP5 are involved in inhibiting JNK.** A, FLAG-JNK-1a1, immunoprecipitated from the cell lysates with the FLAG antibody, was mixed with indicated recombinant 6×His-GST, 6×His-mSH3BP5, or a 6×His-mSH3BP5 deletion mutant (1 μg per sample), and subjected to *in vitro* JNK kinase assays using recombinant c-Jun as a substrate (*top panel*) and to SDS-PAGE and immunoblot analysis (*middle and bottom panels*). Immunoblot analysis was performed with the antibody to phospho c-Jun, the antibody to HisG for the detection of 6×His-tagged recombinant proteins, and the antibody to FLAG for the detection of FLAG-JNK-1a1. B, F11 cells, cotransfected with the empty pFLAG vector (*vector*) or a pFLAG vector encoding mSH3BP5 or an mSH3BP5 deletion mutant together with the empty pcDNA3 vector (*vector*) or pcDNA3-V642I-APP (V642I-APP). At 72 h after transfection, they were harvested for Trypan Blue cell death assays. Cell lysates were subjected to SDS-PAGE and immunoblot analysis with the M2 antibody to FLAG and the APP antibody (22C11). \*\*\*,  $p < 0.001$ ; n.s., not significant.

JNK (Fig. 8C). Two mechanisms may underlie this; 1) overexpressed SH3BP5 binds to JNK and prohibits MKK4/MKK7 from accessing JNK and 2) overexpressed SH3BP5 binds to MKK4/MKK7, another JNK-activating MAPKK, or another

kinase located upstream of JNK, and directly inhibits their kinase activities. Although it remains undefined which, if either, of these mechanisms occurs, it is apparent that overexpressed SH3BP5 inhibits the JNK-activating kinase-mediated

## SH3BP5 Mediates Humanin Activity via JNK

phosphorylation of JNK. This finding on SH3BP5 is in contrast to the finding that JIP-1 enhances the MKK7-induced phosphorylation of JNK (52). It was also reported that the overexpression of SH3BP5 led to the reduction of B cell antigen receptor-induced tyrosine phosphorylation of Btk and significantly reduced both early and late B cell antigen receptor-mediated events (36). This finding suggests that SH3BP5 may inhibit the Btk-mediated signal. It is also possible that SH3BP5 affects other MAP kinase signaling pathways, and this should be addressed in future investigations.

It is highly likely that SH3BP5 is not the single downstream effector of Humanin, for a number of reasons. First, there are so many transcriptional targets for Humanin. Indeed, we identified several other transcriptional target genes of Humanin using differential display screening, some of which may contribute to the neuroprotective effect of Humanin. Second, given that htHNR belongs to the interleukin-6 receptor family, which activates ERK signaling (53), it is likely that the binding of Humanin to htHNR activates intracellular signals via ERK independently of STAT3. Third, phosphoinositide 3 kinase- and Akt-mediated signaling is activated by Humanin in a mouse stroke model (10). Finally, the signals activated by the Humanin binding to Humanin receptors other than htHNR, such as Bax (29) and formyl peptide receptor-like protein 1 (30), may also contribute to the protective effect of Humanin. Each of these aforementioned signals may contribute to the activity of Humanin in a context-dependent manner.

A high-level of SH3BP5 overexpression is sufficient to inhibit V642I-APP-induced neuronal death in F11 neurohybrid cells and SH-SY5Y cells (Figs. 3 and 4). Therefore, if the endogenous expression of SH3BP5, induced by Humanin, reaches the level that is sufficient to inhibit neuronal death, other effectors than SH3BP5 are not necessary in these cells. However, it is quite difficult to determine whether the levels of SH3BP5 overexpression are sufficient or not. Importantly, considering that siRNA-mediated knockdown of endogenous SH3BP5 almost completely inhibited the neuroprotective effect of Humanin in the same cells (Figs. 5 and 6), it is reasonable to conclude that SH3BP5 “centrally” mediates the neuroprotective effect of Humanin in these cells, although other downstream effectors may cooperate with SH3BP5 to exert the neuroprotective effect of Humanin. The level of SH3BP5 expression is not uniform between neurons in distinct brain areas. While it is relatively high in the CA3 region of hippocampus, it is relatively low in both dentate gyrus of hippocampus and cortex (Fig. 2). Consequently, it is possible that SH3BP5 centrally contributes to the effect of Humanin in the CA3 region of hippocampus, whereas it only minimally contributes to the effects in dentate gyrus of hippocampus and cortex.

In this study, the co-immunoprecipitation experiments showed that SH3BP5 bound to JNK through SH3BD, KIM1, and KIM2 (Fig. 9D). This result is not in agreement with the result in the former study (35, 39), where it was shown that SH3BP5 bound to JNK only through KIM1. The discrepancy may be originated from differences in the employed co-precipitation procedure. First, we used 6×His-tagged SH3BP5 deletion mutants, while they used GST-tagged SH3BP5 deletion mutants. Second, we immunoprecipitated FLAG-JNK1a1 with

the FLAG antibody and examined co-precipitated SH3BP5 deletion mutants by immunoblot analysis, while they pulled down GST-tagged SH3BP5 deletion mutants with glutathione beads and examined co-precipitated JNK by immunoblot analysis.

SH3BP5 has been identified to be a downstream effector of Humanin. In a previous study (22), the level of phosphorylated STAT3, an activated STAT3, was reduced in neurons of hippocampus of AD cases, which has led to the assumption that the Humanin signal may be down-regulated there and the down-regulation of the Humanin signal contributes to the AD pathogenesis. If the assumption is true, the level of SH3BP5 may be down-regulated in neurons of hippocampus of AD cases.

In summary, the present study shows that SH3BP5 directly inhibits JNK, and that SH3BP5 is an important downstream effector of Humanin, which contributes to Humanin-induced neuroprotective activity.

---

*Acknowledgments*—We thank Takako Hiraki and Yuka Toyama for technical assistance throughout the study.

---

## REFERENCES

1. Hashimoto, Y., Niikura, T., Tajima, H., Yasukawa, T., Sudo, H., Ito, Y., Kita, Y., Kawasumi, M., Kouyama, K., Doyu, M., Sobue, G., Koide, T., Tsuji, S., Lang, J., Kurokawa, K., and Nishimoto, I. (2001) A rescue factor abolishing neuronal cell death by a wide spectrum of familial Alzheimer's disease genes and A $\beta$ . *Proc. Natl. Acad. Sci. U.S.A.* **98**, 6336–6341
2. Nishimoto, I., Matsuoka, M., and Niikura, T. (2004) Unraveling the role of Humanin. *Trends Mol. Med.* **10**, 102–105
3. Matsuoka, M. (2009) Humanin; a defender against Alzheimer's disease? *Recent. Pat. CNS Drug Discov.* **4**, 37–42
4. Matsuoka, M. (2011) Humanin signal for Alzheimer's disease. *J. Alzheim. Dis.* **24**, 27–32
5. Kariya, S., Takahashi, N., Ooba, N., Kawahara, M., Nakayama, H., and Ueno, S. (2002) Humanin inhibits cell death of serum-deprived PC12h cells. *Neuroreport* **13**, 903–907
6. Kariya, S., Takahashi, N., Hirano, M., and Ueno, S. (2003) Humanin improves impaired metabolic activity and prolongs survival of serum-deprived human lymphocytes. *Mol. Cell. Biochem.* **254**, 83–89
7. Wang, D., Li, H., Yuan, H., Zheng, M., Bai, C., Chen, L., and Pei, X. (2005) Humanin delays apoptosis in K562 cells by downregulation of P38 MAP kinase. *Apoptosis* **10**, 963–971
8. Hoang, P. T., Park, P., and Cobb, L. J., Paharkova-Vatchkova, V., Hakimi, M., Cohen, P., and Lee, K. W. (2010) The neurosurvival factor Humanin inhibits  $\beta$ -cell apoptosis via signal transducer and activator of transcription 3 activation and delays and ameliorates diabetes in nonobese diabetic mice. *Metabolism* **59**, 343–349
9. Colón, E., Strand, M. L., Carlsson-Skewir, C., Wahlgren, A., Svechnikov, K. V., Cohen, P., and Söder, O. (2006) Anti-apoptotic factor humanin is expressed in the testis and prevents cell-death in Leydig cells during the first wave of spermatogenesis. *J. Cell. Physiol.* **208**, 373–385
10. Xu, X., Chua, C. C., Gao, J., Hamdy, R. C., and Chua, B. H. (2006) Humanin is a novel neuroprotective agent against stroke. *Stroke* **7**, 2613–2619
11. Xu, X., Chua, C. C., Gao, J., Chua, K. W., Wang, H., Hamdy, R. C., and Chua, B. H. (2008) Neuroprotective effect of humanin on cerebral ischemia/reperfusion injury is mediated by a PI3K/Akt pathway. *Brain Res.* **1227**, 12–18
12. Lue, Y., Swerdloff, R., Liu, Q., Mehta, H., Hikim, A. S., Lee, K. W., Jia, Y., Hwang, D., Cobb, L. J., Cohen, P., and Wang, C. (2010) Opposing roles of insulin-like growth factor binding protein 3 and humanin in the regulation of testicular germ cell apoptosis. *Endocrinology* **151**, 350–357
13. Muzumdar, R. H., Huffman, D. M., Calvert, J. W., Jha, S., Weinberg, Y.,

- Cui, L., Nemkal, A., Atzmon, G., Klein, L., Gundewar, S., Ji, S. Y., Lavu, M., Predmore, B. L., and Lefer, D. J. (2010) Acute humanin therapy attenuates myocardial ischemia and reperfusion injury in mice. *Arterioscler. Thromb. Vasc. Biol.* **30**, 1940–1948
14. Bachar, A. R., Scheffer, L., Schroeder, A. S., Nakamura, H. K., Cobb, L. J., Oh, Y. K., Lerman, L. O., Pagano, R. E., Cohen, P., and Lerman, A. (2010) Humanin is expressed in human vascular walls and has a cytoprotective effect against oxidized LDL-induced oxidative stress. *Cardiovasc. Res.* **88**, 360–366
  15. Mamiya, T., and Ukai, M. (2001) [Gly(14)]-Humanin improved the learning and memory impairment induced by scopolamine *in vivo*. *Br. J. Pharmacol.* **134**, 1597–1599
  16. Krejcova, G., Patocka, J., and Slaninova, J. (2004) Effect of humanin analogues on experimentally induced impairment of spatial memory in rats. *J. Pept. Sci.* **10**, 636–639
  17. Kunesová, G., Hlaváček, J., Patocka, J., Evangelou, A., Zikos, C., Benaki, D., Paravatou-Petsotas, M., Pelecanou, M., Livaniou, E., and Slaninova, J. (2008) The multiple T-maze *in vivo* testing of the neuroprotective effect of humanin analogues. *Peptides* **29**, 1982–1987
  18. Yamada, M., Chiba, T., Sasabe, J., Nawa, M., Tajima, H., Niikura, T., Terashita, K., Aiso, S., Kita, Y., Matsuoka, M., and Nishimoto, I. (2005) Implanted cannula-mediated repetitive administration of A $\beta$ 25–35 into the mouse cerebral ventricle effectively impairs spatial working memory. *Behav. Brain Res.* **164**, 139–146
  19. Tajima, H., Kawasumi, M., Chiba, T., Yamada, M., Yamashita, K., Nawa, M., Kita, Y., Kouyama, K., Aiso, S., Matsuoka, M., Niikura, T., and Nishimoto, I. (2005) A humanin derivative, S14G-HN, prevents amyloid- $\beta$ -induced memory impairment in mice. *J. Neurosci. Res.* **79**, 714–723
  20. Chiba, T., Yamada, M., Hashimoto, Y., Sato, M., Sasabe, J., Kita, Y., Terashita, K., Aiso, S., Nishimoto, I., and Matsuoka, M. (2005) Development of a femtomolar-acting humanin derivative named colivelin by attaching activity-dependent neurotrophic factor to its N terminus: characterization of colivelin-mediated neuroprotection against Alzheimer's disease-relevant insults *in vitro* and *in vivo*. *J. Neurosci.* **25**, 10252–10261
  21. Miao, J., Zhang, W., Yin, R., Liu, R., Su, C., Lei, G., and Li, Z. (2008) S14G-Humanin ameliorates A $\beta$ 25–35-induced behavioral deficits by reducing neuroinflammatory responses and apoptosis in mice. *Neuropeptides* **42**, 557–567
  22. Chiba, T., Yamada, M., Sasabe, J., Terashita, K., Shimoda, M., Matsuoka, M., and Aiso, S. (2009) Amyloid- $\beta$  causes memory impairment by disturbing the JAK2/STAT3 axis in hippocampal neurons. *Mol. Psychiatry* **14**, 206–222
  23. Niikura, T., Sidahmed, E., Hirata-Fukae, C., Aisen, P.S., and Matsuoka, Y. (2011) A humanin derivative reduces amyloid  $\beta$  accumulation and ameliorates memory deficit in triple transgenic mice. *PLoS One* **6**, e16259
  24. Zhang, W., Zhang, W., Li, Z., Hao, J., Zhang, Z., Liu, L., Mao, N., Miao, J., and Zhang, L. (2012) S14G-humanin improves cognitive deficits and reduces amyloid pathology in the middle-aged APPswe/PS1dE9 mice. *Pharmacol. Biochem. Behav.* **100**, 361–369
  25. Ashe, K. H., and Zahs, K. R. (2010) Probing the biology of Alzheimer's disease in mice. *Neuron* **66**, 631–645
  26. Muzumdar, R. H., Huffman, D. M., Atzmon, G., Buettner, C., Cobb, L. J., Fishman, S., Budagov, T., Cui, L., Einstein, F. H., Poduval, A., Hwang, D., Barzilai, N., and Cohen, P. (2009) Humanin: a novel central regulator of peripheral insulin action. *PLoS One* **4**, e6334
  27. Oh, Y. K., Bachar, A. R., Zacharias, D. G., Kim, S. G., Wan, J., Cobb, L. J., Lerman, L. O., Cohen, P., and Lerman, A. (2011) Humanin preserves endothelial function and prevents atherosclerotic plaque progression in hypercholesterolemic ApoE-deficient mice. *Atherosclerosis* **219**, 65–73
  28. Matsuoka, M., and Hashimoto, Y. (2010) Humanin and the receptors for humanin. *Mol. Neurobiol.* **41**, 22–28
  29. Guo, B., Zhai, D., Cabezas, E., Welsh, K., Nouraini, S., Satterthwait, A. C., and Reed, J. C. (2003) Humanin peptide suppresses apoptosis by interfering with Bax activation. *Nature* **423**, 456–461
  30. Ying, G., Iribarren, P., Zhou, Y., Gong, W., Zhang, N., Yu, Z. X., Le, Y., Cui, Y., and Wang, J. M. (2004) Humanin, a newly identified neuroprotective factor, uses the G protein-coupled formylpeptide receptor-like-1 as a functional receptor. *J. Immunol.* **172**, 7078–7085
  31. Hashimoto, Y., Kurita, M., Aiso, S., Nishimoto, I., and Matsuoka, M. (2009) Humanin inhibits neuronal cell death by interacting with a cytokine receptor complex or complexes involving CNTF receptor  $\alpha$ /WSX-1/gp130. *Mol. Biol. Cell* **20**, 2864–2873
  32. Hashimoto, Y., Kurita, M., and Matsuoka, M. (2009) Identification of soluble WSX-1 not as a dominant-negative but as an alternative functional subunit of a receptor for an anti-Alzheimer's disease rescue factor Humanin. *Biochem. Biophys. Res. Commun.* **389**, 95–99
  33. Hashimoto, Y., Suzuki, H., Aiso, S., Niikura, T., Nishimoto, I., and Matsuoka, M. (2005) Involvement of tyrosine kinases and STAT3 in Humanin-mediated neuroprotection. *Life Sci.* **77**, 3092–3104
  34. Matsushita, M., Yamadori, T., Kato, S., Takemoto, Y., Inazawa, J., Baba, Y., Hashimoto, S., Sekine, S., Arai, S., Kunikata, T., Kurimoto, M., Kishimoto, T., and Tsukada, S. (1998) Identification and characterization of a novel SH3-domain binding protein, Sab, which preferentially associates with Bruton's tyrosine kinase (Btk). *Biochem. Biophys. Res. Commun.* **245**, 337–343
  35. Wiltshire, C., Matsushita, M., Tsukada, S., Gillespie, D. A., and May, G. H. (2002) A new c-Jun N-terminal kinase (JNK)-interacting protein, Sab (SH3BP5), associates with mitochondria. *Biochem. J.* **236**, 577–585
  36. Yamadori, T., Baba, Y., Matsushita, M., Hashimoto, S., Kurosaki, M., Kurosaki, T., Kishimoto, T., and Tsukada, S. (1999) Bruton's tyrosine kinase activity is negatively regulated by Sab, the Btk-SH3 domain-binding protein. *Proc. Natl. Acad. Sci. U.S.A.* **196**, 6341–6346
  37. Hashimoto, Y., Tsuji, O., Niikura, T., Yamagishi, Y., Ishizaka, M., Kawasumi, M., Chiba, T., Kanekura, K., Yamada, M., Tsukamoto, E., Kouyama, K., Terashita, K., Aiso, S., Lin, A., and Nishimoto, I. (2003) Involvement of c-Jun N-terminal kinase in amyloid precursor protein-mediated neuronal cell death. *J. Neurochem.* **84**, 864–877
  38. Hashimoto, Y., Niikura, T., Chiba, T., Tsukamoto, E., Kadowaki, H., Nishitoh, H., Yamagishi, Y., Ishizaka, M., Yamada, M., Nawa, M., Terashita, K., Aiso, S., Ichijo, H., and Nishimoto, I. (2003) The cytoplasmic domain of Alzheimer's amyloid- $\beta$  protein precursor causes sustained apoptosis signal-regulating kinase 1/c-Jun NH2-terminal kinase-mediated neurotoxic signal via dimerization. *J. Pharmacol. Exp. Ther.* **306**, 889–902
  39. Wiltshire, C., Gillespie, D. A., and May, G. H. (2004) Sab (SH3BP5), a novel mitochondria-localized JNK-interacting protein. *Biochem. Soc. Trans.* **2**, 1075–1077
  40. Sui, G., Soohoo, C., Affar, el B., Gay, F., Shi, Y., Forrester, W. C., and Shi, Y. (2002) A DNA vector-based RNAi technology to suppress gene expression in mammalian cells. *Proc. Natl. Acad. Sci. U.S.A.* **99**, 5515–5520
  41. Yamatsui, T., Matsui, T., Okamoto, T., Komatsuzaki, K., Takeda, S., Fukumoto, H., Iwatsubo, T., Suzuki, N., Asami-Odaka, A., Ireland, S., Kinane, T. B., Giambarella, U., and Nishimoto, I. (1996) G protein-mediated neuronal DNA fragmentation induced by familial Alzheimer's disease-associated mutants of APP. *Science* **272**, 1349–1352
  42. Tachi, N., Hashimoto, Y., and Matsuoka, M. (2012) MOCA is an integrator of the neuronal death signals that are activated by familial Alzheimer's disease-related mutants of amyloid  $\beta$  precursor protein and presenilins. *Biochem. J.* **442**, 413–422
  43. Niikura, T., Hashimoto, Y., Tajima, H., and Nishimoto, I. (2002) Death and survival of neuronal cells exposed to Alzheimer's insults. *J. Neurosci. Res.* **70**, 380–391
  44. Kawasumi, M., Hashimoto, Y., Chiba, T., Kanekura, K., Yamagishi, Y., Ishizaka, M., Tajima, H., Niikura, T., and Nishimoto, I. (2002) Molecular mechanisms for neuronal cell death by Alzheimer's amyloid precursor protein-relevant insults. *Neurosignals* **11**, 236–250
  45. Dhanasekaran, D. N., and Reddy, E. P. (2008) JNK signaling in apoptosis. *Oncogene* **27**, 6245–6251
  46. Chambers, J. W., Cherry, L., Laughlin, J. D., Figueroa-Losada, M., and Lograsso, P. V. (2011) Selective inhibition of mitochondrial JNK signaling achieved using peptide mimicry of the Sab kinase interacting motif-1 (KIM1). *ACS Chem. Biol.* **6**, 808–818
  47. Win, S., Than, T. A., Han, D., Petrovic, L. M., and Kaplowitz, N. (2011) c-Jun N-terminal kinase (JNK)-dependent acute liver injury from acetaminophen or tumor necrosis factor (TNF) requires mitochondrial Sab protein expression in mice. *J. Biol. Chem.* **286**, 35071–35078
  48. Chambers, J. W., Howard, S., and LoGrasso, P. V. (2013) Blocking c-Jun-

## SH3BP5 Mediates Humanin Activity via JNK

- N-terminal kinase (JNK) translocation to the mitochondria prevents 6-hydroxydopamine-induced toxicity in vitro and in vivo. *J. Biol. Chem.* **288**, 1079–1087
49. Chambers, J. W., Pachori, A., Howard, S., Iqbal, S., and LoGrasso, P. V. (2013) Inhibition of JNK mitochondrial localization and signaling is protective against ischemia/reperfusion injury in rats. *J. Biol. Chem.* **288**, 4000–4011
50. Brown, D. I., and Griendling, K. K. (2009) Nox proteins in signal transduction. *Free Radic. Biol. Med.* **47**, 1239–1253
51. Dickens, M., Rogers, J. S., Cavanagh, J., Raitano, A., Xia, Z., Halpern, J. R., Greenberg, M. E., Sawyers, C. L., and Davis, R. J. (1997) A cytoplasmic inhibitor of the JNK signal transduction pathway. *Science* **277**, 693–696
52. Whitmarsh, A. J., Cavanagh, J., Tournier, C., Yasuda, J., and Davis R. J. (1998) A mammalian scaffold complex that selectively mediates MAP kinase activation. *Science* **281**, 1671–1674
53. Ohtani, T., Ishihara, K., Atsumi, T., Nishida, K., Kaneko, Y., Miyata, T., Itoh, S., Narimatsu, M., Maeda, H., Fukada, T., Itoh, M., Okano, H., Hibi, M., and Hirano, T. (2000) Dissection of signaling cascades through gp130 *in vivo*: reciprocal roles for STAT3- and SHP2-mediated signals in immune responses. *Immunity* **12**, 95–105